

1
2
3
4
5
6
7
8
9
10
11
12
13
14
15
16
17
18

Physiological responses of coastal and oceanic diatoms to diurnal fluctuations in seawater carbonate chemistry under two CO₂ concentrations

Running head: ocean acidification influences diatoms under fluctuating pH

Futian Li¹, Yaping Wu¹, David A. Hutchins², Feixue Fu², and Kunshan Gao^{1*}

¹State Key Laboratory of Marine Environmental Science, Xiamen University, Xiamen 361102, China

²Department of Biological Sciences, University of Southern California, Los Angeles, California, United States of America

*Corresponding author e-mail: ksgao@xmu.edu.cn (Kunshan Gao)

19 **Abstract**

20 Diel and seasonal fluctuations in seawater carbonate chemistry are common in coastal waters, while
21 in the open ocean carbonate chemistry is much less variable. In both of these environments, ongoing
22 ocean acidification is being superimposed on the natural dynamics of the carbonate buffer system to
23 influence the physiology of phytoplankton. Here, we show that a coastal *Thalassiosira weissflogii*
24 isolate and an oceanic diatom, *Thalassiosira oceanica*, respond differentially to diurnal fluctuating
25 carbonate chemistry in current and ocean acidification (OA) scenarios. A fluctuating carbonate
26 chemistry regime showed positive or negligible effects on physiological performance of the coastal
27 species. In contrast, the oceanic species was significantly negatively affected. The fluctuating regime
28 reduced photosynthetic oxygen evolution rates and enhanced dark respiration rates of *T. oceanica* under
29 ambient CO₂ concentration, while in the OA scenario, the fluctuating regime depressed its growth rate,
30 chlorophyll *a* content, and elemental production rates. These contrasting physiological performances of
31 coastal and oceanic diatoms indicate that they differ in the ability to cope with dynamic *p*CO₂. We
32 propose that, in addition to the ability to cope with light, nutrient, and predation pressure, the ability to
33 acclimate to dynamic carbonate chemistry may act as one determinant of the spatial distribution of
34 diatom species. Habitat-relevant diurnal changes in seawater carbonate chemistry can interact with OA
35 to differentially affect diatoms in coastal and pelagic waters.

36

37

38

39

40

41

42

43 **Key words:** diatom, growth, photosynthesis, elemental production rates, fluctuating carbonate
44 chemistry, CO₂

45

46 **1 Introduction**

47 Anthropogenic emissions of carbon dioxide (CO₂) since the industrial revolution have increased
48 atmospheric *p*CO₂ levels by 40% (Howes et al. 2015), mainly due to burning of fossil fuels and land use
49 changes (Ciais et al. 2014). The oceans absorb about 30% of the CO₂ emitted by human activities
50 (Sabine et al. 2004), leading to decreases in pH, concentration of carbonate ions, and saturation state of
51 calcium carbonate, along with increases of the concentrations of aqueous CO₂ and bicarbonate (i.e.,
52 ocean acidification). The global surface ocean mean pH has already decreased by about 0.1 units since
53 the industrial revolution (Orr et al. 2005; Doney 2010), and a further decrease of 0.3-0.4 units is
54 expected to happen by 2100 under the business as usual scenario (Orr et al. 2005; Gattuso et al. 2015).

55 For marine organisms, the reduced seawater mean pH caused by ocean acidification (OA) could be
56 detectable on a timescale of years to decades, while striking fluctuations in coastal seawater carbonate
57 chemistry may occur over much shorter timescales in current and OA scenarios. The coastal zone plays
58 a critical role in biogeochemical cycles, and experiences great variability of physical and chemical
59 factors (Drupp et al. 2011). In addition, it is the area most impacted by anthropogenic pressures (Gattuso
60 et al. 1998). Carbonate chemistry in coastal seawater is affected by multiple drivers in addition to
61 atmospheric CO₂ dissolution, such as tidal cycles (Dai et al. 2009; Jiang et al. 2011; Wang et al. 2014),
62 upwelling (Feely et al. 2008; Capone and Hutchins 2013), watershed processes, wind forcing (Drupp et
63 al. 2011), anthropogenic nutrient inputs, aquaculture activities, and changes in ecosystem structure and
64 metabolism (Duarte et al. 2013; Waldbusser and Salisbury 2014). Due to high biomass and sufficient or
65 excess nutrients in coastal waters, biological activities alter *p*CO₂, resulting in a diel cycle of pH. The
66 diel range of pH variation in some coastal ecosystems can be greater than 1 pH unit (Duarte et al. 2013),
67 which corresponds to a 900% change in H⁺ concentration.

68 During a diurnal cycle, organisms in coastal areas could experience pH values that may be lower than
69 the projected value for the surface ocean in the year 2100 (Hofmann et al. 2011; Hurd et al. 2011;
70 Waldbusser and Salisbury 2014). In contrast, pH in the open ocean is relatively stable, with a variation
71 range of only ~ 0.024 over a month (Hofmann et al. 2011). Considering the lower buffering capacity in
72 the OA scenario, pH variability would increase in both coastal and oceanic waters (Egleston et al. 2010;

73 Cai et al. 2011; Denman et al. 2011; Wang et al. 2013). The amplitude of pH variation in coastal water
74 will be larger than in oceanic water due to the presence of multiple drivers (Waldbusser and Salisbury
75 2014). For instance, biological activities could increase variation in pH up to 40% compared to the
76 present extent of variation under elevated $p\text{CO}_2$ conditions in coastal waters (Egleston et al. 2010).

77 Responses of fish (Dixon 2014), gastropods (Onitsuka et al. 2014), oysters (Keppel 2015), mussels
78 (Frieder et al. 2014), coral (Dufault et al. 2012; Comeau et al. 2014), canopy-forming kelp (Britton et al.
79 2016), and coralline algae (Gao et al. 1993; Cornwall et al. 2013; Noisette et al. 2013; Johnson et al.
80 2014) to diurnally fluctuating $p\text{CO}_2/\text{pH}$ have been studied recently. Dufault et al. (2012) hypothesized
81 that storage of dissolved inorganic carbon during the night-time high $p\text{CO}_2$ period fueled day-time
82 calcification (and perhaps photosynthesis), resulting in higher calcification and survival rate of coral
83 recruits. Thus, it appears that some marine organisms may benefit from $p\text{CO}_2$ fluctuations. In spite of
84 this body of literature, the responses of marine phytoplankton to fluctuating pH/ $p\text{CO}_2$ are still unclear.
85 To our knowledge, only one study has addressed the responses of the marine green alga *Ostreococcus* to
86 fluctuating $p\text{CO}_2$ (Schaum et al. 2016). However, how CO_2 variability affects other major marine
87 phytoplankton groups over either the short- or long-term remains unknown.

88 Coastal and open ocean species are distinguished by habitat-related differences in cell size, nutrient
89 utilization (Glibert and Ray 1990), photosynthetic architecture (Strzepek and Harrison 2004), and
90 photosynthetic performance (Lavaud et al. 2007; Li et al. 2011; Liu and Qiu 2012). Our study was
91 intended to understand whether coastal and oceanic species also differ in their capacity to respond to
92 fluctuating carbonate chemistry. A coastal *Thalassiosira weissflogii* isolate and an oceanic diatom,
93 *Thalassiosira oceanica*, were used in the present study. We manipulated $p\text{CO}_2$ to mimic diurnally
94 fluctuating carbonate chemistry and hypothesized that coastal diatoms would show better physiological
95 performance under fluctuating carbonate chemistry than oceanic ones, a difference that could
96 potentially be a key factor influencing the geographical distribution of diatoms.

97

98 **2 Materials and methods**

99 **2.1 Cultures and experimental setup**

100 *Thalassiosira weissflogii* (CCMP 1336, isolated from coastal Long Island, New York, USA in 1956)
101 and *Thalassiosira oceanica* (CCMP 1005, isolated from the Sargasso Sea in 1958) were incubated in
102 Aquil medium (Sunda et al. 2005). Triplicate cultures (incubated in 1 L autoclaved Erlenmeyer flasks)
103 were used for each treatment, illuminated by cool white fluorescent light at an intensity of 115 μmol
104 $\text{photons m}^{-2} \text{s}^{-1}$. Cultures were maintained at 20 °C with a 12 h:12 h light and dark cycle. Cells were
105 maintained at exponential growth phase with maximal concentration $< 1.1 \times 10^4 \text{ mL}^{-1}$ (*T. weissflogii*) or
106 $3.5 \times 10^4 \text{ mL}^{-1}$ (*T. oceanica*) in semi-continuous cultures (cultures were diluted every 24 h at 6 h after
107 the onset of light).

108 *T. weissflogii* and *T. oceanica* were acclimated to four treatments: 1) steady carbonate chemistry at
109 ambient $p\text{CO}_2$ level (LCs); 2) diurnally carbonate chemistry fluctuated around ambient $p\text{CO}_2$ level
110 (LCf); 3) steady carbonate chemistry at elevated $p\text{CO}_2$ level (HCs); and 4) diurnally carbonate
111 chemistry fluctuated around elevated $p\text{CO}_2$ level (HCf) for 15 generations before sampling. Steady
112 regimes were bubbled with ambient air ($400 \pm 15 \mu\text{atm}$, LCs) or elevated ($1005 \pm 40 \mu\text{atm}$, HCs) $p\text{CO}_2$,
113 which was automatically achieved by mixing air/ CO_2 with a CO_2 Enricher (CE100B, RuiHua). The
114 fluctuating regimes were obtained by changing the CO_2 partial pressure every 12 h. Cells were aerated
115 with air of low $p\text{CO}_2$ (i.e., 0 or $557 \pm 15 \mu\text{atm}$ for Lcf and HCf, respectively) during the photoperiod;
116 the aeration was changed to high $p\text{CO}_2$ (i.e., 870 ± 19 or $1949 \pm 35 \mu\text{atm}$ for Lcf and HCf, respectively)
117 at the beginning of the dark period. Measurements showed that pH gradually increased and decreased,
118 similar to a natural diurnal cycle (see Results). Since pH increased quickly in the first few hours of the
119 photoperiod, the aeration rates were adjusted to make sure the fluctuating regimes reached similar pH
120 values with corresponding steady regimes in the middle of photoperiod and reached target values at the
121 end of photoperiod. The steady regimes were aerated with stable $p\text{CO}_2$ air at the same flow rate as the
122 fluctuating regimes. The pH was measured every 1.5 h by a pH meter (Orion 2 STAR, Thermo
123 Scientific) calibrated with standard National Bureau of Standards (NBS) buffers. Samples for total
124 alkalinity (TA) measurement were poisoned with a saturated solution of mercuric chloride after
125 filtration. TA was determined by Gran acidimetric titration with a TA analyzer (AS-ALK1+, Apollo
126 SciTech). Certified reference materials obtained from A. G. Dickson at the Scripps Institution of

127 Oceanography were used to assure the accuracy of the TA measurement. TA and pH were applied to
128 CO2SYS software to calculate other carbonate chemistry parameters (Table 1). Subsamples for
129 measurement of physiological parameters were always taken in the middle of the photoperiod (6 h after
130 the onset of light), unless otherwise noted.

131

132 **2.2 Growth rate and chlorophyll *a* content**

133 Cell concentration and mean cell size were measured by a Coulter Particle Count and Size Analyzer
134 (Z2, Beckman Coulter). Specific growth rate was calculated according the equation:

135 $\mu = (\ln N_1 - \ln N_0) / (t_1 - t_0)$, in which N_1 and N_0 represent cell concentrations at t_1 and t_0 . For the

136 chlorophyll *a* content determination, samples were filtered onto GF/F filters (25 mm, Whatman), and
137 extracted overnight at 4 °C in absolute methanol before centrifugation. The supernatants were analyzed
138 by a UV-VIS Spectrophotometer (DU800, Beckman Coulter) and the chlorophyll *a* content was
139 calculated according to the equation of Ritchie (2006).

140

141 **2.3 Elemental composition and production rate**

142 Samples for measuring particulate organic carbon (POC) and nitrogen (PON) were filtered onto pre-
143 combusted (450 °C for 6 h) GF/F filters (25 mm, Whatman). Filters were treated using HCl fumes to
144 remove any inorganic carbon and dried before analysis on a CHNS/O Analyzer (2400SeriesII,
145 PerkinElmer). Polycarbonate filters (1.2 μm pore size) were used to determine biogenic silica (BSi) by
146 the spectrophotometric method of Brzezinski and Nelson (1995). Production rates of POC, PON, and
147 BSi were calculated by multiplying cellular content by specific growth rate.

148

149 **2.4 Chlorophyll *a* fluorescence**

150 The photochemical parameters were determined using a Xenon-Pulse Amplitude Modulated
151 fluorometer (Xe-PAM, Walz). Effective photochemical quantum yields were determined according to
152 the equation of Genty et al. (1989): $\Phi_{PSII} = (F_m' - F_t) / F_m' = \Delta F / F_m'$ for light-adapted samples, where
153 F_m' indicates maximum chlorophyll fluorescence of light-adapted samples, and F_t , steady chlorophyll

154 fluorescence of light-adapted samples. Non-photochemical quenching (NPQ) was calculated as: $NPQ =$
155 $(F_m - F_m') / F_m'$, where F_m indicates maximum chlorophyll fluorescence of dark-adapted samples. Φ_{PSII}
156 and NPQ were measured under actinic light intensity ($\sim 156 \mu\text{mol photons m}^{-2} \text{ s}^{-1}$) similar to culture
157 light level after 10 min dark adaptation. Given the changing carbonate chemistry over a diurnal cycle,
158 Φ_{PSII} and NPQ were determined at three time points: 0.5, 6, and 11.5 h after the onset of light.

159

160 **2.5 Photosynthetic oxygen evolution and dark respiration rates**

161 Net photosynthetic oxygen evolution and dark respiration rates were determined using a Clark-type
162 oxygen electrode (Oxygraph, Hansatech) at the experimental temperature. Oxygen evolution rates were
163 measured under $115 \mu\text{mol photons m}^{-2} \text{ s}^{-1}$ at the same three time points as mentioned above. Oxygen
164 consumption rates were measured in the middle of photoperiod (6 h after the onset of light), when the
165 steady and fluctuating regimes reached similar pH values. Samples were gently filtered ($< 0.02 \text{ MPa}$)
166 onto 47 mm cellulose acetate membranes, and then re-suspended into 20 mmol L^{-1} Tris buffered
167 medium. The re-suspended cells were injected into an oxygen electrode chamber equipped with a
168 magnetic stirrer. Rates of oxygen evolution and consumption were derived from the linear portion of the
169 slope of the oxygen record ($\sim 10 \text{ min per sample}$). The pH values of Tris buffered media were pre-
170 adjusted to their corresponding culture media values. That is, pH values of Tris buffered media of the
171 three time points in the LCf treatment were 7.84, 8.14, and 8.35, and those in the HCf treatment were
172 7.54, 7.80, and 8.06. Values in the LCs and HCs treatments were set to 8.14 or 7.80 for all three time
173 points, respectively.

174

175 **2.6 Statistical analyses**

176 Data were analyzed by a two-way analysis of variance (ANOVA) with $p\text{CO}_2$ level and $p\text{CO}_2$
177 variability classed as factors in the model, each with two levels ($400 \pm 15 \mu\text{atm}$, $1005 \pm 40 \mu\text{atm}$; and
178 steady, fluctuating $p\text{CO}_2$, respectively). The interaction of the two factors was also included in the
179 model. All data used for ANOVA analysis were tested for normality (Shapiro-Wilk test) and
180 homogeneity of variances (Levene test). When p values were under 0.05, the post hoc Duncan test was

181 used to determine the differences between treatments. All data are reported as mean value of triplicate
182 cultures \pm standard deviation (SD).

183

184 **3 Results**

185 **3.1 Variation of pH in experimental regimes**

186 The variation ranges of pH in the LCf and HCf treatments were 0.52 ± 0.03 , and 0.53 ± 0.03 ,
187 respectively. At the beginning of the photoperiod, pH of the LCf regime was 7.84 ± 0.02 (Fig. 1), and
188 then it increased to 8.15 ± 0.03 at 6 h after the onset of light, similar to the value of the LCs regime
189 (8.13 ± 0.02). The pH value of the LCf regime reached 8.35 ± 0.02 at 12 h after the onset of light, and
190 then decreased to 7.84 ± 0.02 . For the HCf regime, pH ranged from 7.54 ± 0.01 to 8.06 ± 0.02 , and
191 reached 7.82 ± 0.01 at 6 h after the onset of light, similar to the value of the HCs regime (7.79 ± 0.01).

192

193 **3.2 Specific growth rate and mean cell size**

194 Growth rates of *T. weissflogii* were not influenced by diurnally fluctuating carbonate chemistry in
195 either the current or the OA scenario (Fig. 2a). No effects of OA on growth rate of *T. weissflogii* were
196 detected. There were no differences in growth rates between the steady and fluctuating regimes for *T.*
197 *oceanica* under the ambient $p\text{CO}_2$ condition (Fig. 2b). However, the fluctuating regime reduced its
198 growth rate by 9% under the elevated $p\text{CO}_2$ condition. OA influenced the growth rate of *T. oceanica*,
199 with rates of HCs cells being 16% lower than those of LCs cells. A significant interaction between
200 $p\text{CO}_2$ level and $p\text{CO}_2$ variability on growth rate of *T. oceanica* was found.

201 Mean cell sizes were not affected by the fluctuating treatment under either ambient or elevated $p\text{CO}_2$
202 conditions in *T. weissflogii* (Table 2). *T. oceanica* cells showed minor but significant changes in cell size
203 in the fluctuating treatments. Cells in the LCf treatment cells were 1.2% larger than LCs cells, while
204 HCf cells were 1.4% smaller than cells in the corresponding steady treatments, resulting in a significant
205 interaction between $p\text{CO}_2$ level and $p\text{CO}_2$ variability.

206

207 **3.3 Chlorophyll *a* content and elemental composition**

208 Chlorophyll *a* contents of *T. weissflogii* in the four treatments were not significantly different. For *T.*
209 *oceanica*, the fluctuating regime didn't influence chlorophyll *a* content under ambient CO₂ level.
210 However, in the HCf treatment chlorophyll *a* content decreased by 24% compared to the steady regime
211 (Table 2). A significant interaction between *p*CO₂ level and *p*CO₂ variability on chlorophyll *a* content of
212 *T. oceanica* was found.

213 POC and PON quotas of both species were elevated in the OA scenario in both the steady and
214 fluctuating regimes, relative to present day *p*CO₂ levels (Table 2). However, no effects of the fluctuating
215 regime on cellular POC and PON contents were detected in either species compared to the steady
216 treatments. The only exception was that POC increased by 9% in the LCf treatment relative to the LCs
217 treatment for *T. weissflogii*. Generally, elevated *p*CO₂ and the fluctuating regime showed no effects on
218 BSi quota of either species, besides a slight decrease in the HCf treatment relative to that of the HCs
219 treatment for *T. weissflogii*.

220 The fluctuating regime increased the POC production rate of *T. weissflogii* at both ambient and
221 elevated *p*CO₂ levels, but had no effects on other elemental production rates of this species. By contrast,
222 the fluctuating regime decreased all of the elemental production rates in the OA scenario for *T. oceanica*
223 (Fig. 3). Significant interactions between *p*CO₂ level and *p*CO₂ variability on elemental production rates
224 of *T. oceanica* were found. Slight but significant decreases of the Si:C ratio in the fluctuating regime
225 compared to the steady regime were found at ambient *p*CO₂ for both species (Table 2). The Si:C ratio of
226 *T. weissflogii* was lower in the OA scenario, and C:N ratios of *T. weissflogii* were not significant
227 different among the four treatments. For *T. oceanica*, cells showed lower C:N and Si:C ratios at elevated
228 *p*CO₂ relative to cells grown at ambient *p*CO₂.

229

230 **3.4 Chlorophyll *a* fluorescence**

231 The effective photochemical quantum yields of both species varied little at different time points,
232 ranging from 0.54 ± 0.03 to 0.61 ± 0.03 among treatments (Table 3). Fluctuating regimes scarcely
233 influenced Φ_{PSII} of either species. The only exception was that Φ_{PSII} of HCf decreased by 8% relative to
234 that of the HCs for *T. weissflogii* at 0.5 h after the onset of light. Elevated *p*CO₂ decreased Φ_{PSII} by 3%

235 and 2% for *T. weissflogii* at 6 and 11.5 h after the onset of light, respectively. *T. oceanica* cells under
236 elevated $p\text{CO}_2$ showed 5% and 7% lower Φ_{PSII} compared to those under ambient $p\text{CO}_2$ at 6 and 11.5 h
237 after the onset of light, respectively. NPQ under culture light intensity ranged from 0.06 ± 0.01 to $0.23 \pm$
238 0.05 at different time points. No detectable effects of the fluctuating regime on NPQ of either species
239 were found, with the exceptions of HCf cells of *T. weissflogii* at 0.5 h after the onset of light and LCf
240 cells of *T. oceanica* 11.5 h after the onset of light. For steady regimes, elevated $p\text{CO}_2$ showed no
241 detectable effect on NPQ of both species at 0.5 h after the onset of light, while it increased NPQ of *T.*
242 *weissflogii* by 37.5% and decreased it by 25% relative to values of LCs cells at 6 and 11.5 h after the
243 onset of light, respectively. Values of NPQ of *T. oceanica* HCs cells were enhanced by 38.4% and
244 decreased by 33.3% relative to values of LCs cells at 6 and 11.5 h after the onset of light, respectively.

245

246 **3.5 Photosynthetic oxygen evolution and dark respiration rates**

247 Chlorophyll normalized net oxygen evolution rates of these two species ranged from 0.39 ± 0.07 to
248 $0.55 \pm 0.07 \mu\text{mol O}_2 \mu\text{g chl } a^{-1} \text{ h}^{-1}$ at 6 h after the onset of light. Neither elevated $p\text{CO}_2$ nor the
249 fluctuating regime showed detectable effects on oxygen evolution rates per chlorophyll of *T. weissflogii*
250 (Fig. 4a), while *T. oceanica* cells under the LCf treatment showed a 29% lower chlorophyll-normalized
251 net oxygen evolution rate relative to the LCs cells (Fig. 4b). A significant interaction between $p\text{CO}_2$
252 level and $p\text{CO}_2$ variability on chlorophyll normalized net oxygen evolution rate of *T. oceanica* was
253 found.

254 Both species, regardless of treatment, showed a similar diurnal rhythm of photosynthetic oxygen
255 evolution: oxygen evolution rates reached the highest values at 6 h after the onset of light (Fig. 4c, d).
256 For *T. weissflogii*, effects of fluctuating $p\text{CO}_2$ on net oxygen evolution per cell were only observed at 6
257 h after the onset of light for cells at the ambient $p\text{CO}_2$ level, with 7% lower rates in the LCf treatment
258 than in the LCs (Fig. 4c). These effects were more obvious for *T. oceanica* cells. *T. oceanica* cells in the
259 steady regime under elevated $p\text{CO}_2$ evolved oxygen at 65% higher cell-specific rates than those in the
260 fluctuating regime at 0.5 h after the onset of light (Fig. 4d). At 11.5 h after the onset of light, LCs cells
261 of *T. oceanica* showed 41% higher net oxygen evolution rates per cell than LCf cells. There were no

262 differences in photosynthetic oxygen evolution rates between HCs and HCf cells 11.5 h after the onset
263 of light.

264 Elevated $p\text{CO}_2$ increased dark respiration of *T. weissflogii* by 57% compared to that at ambient $p\text{CO}_2$
265 level, while the fluctuating regime had no detectable effect (Fig. 5a). In contrast, dark respiration rates
266 of *T. oceanica* were stimulated by 60% for cells under the fluctuating regime compared to steady one at
267 ambient $p\text{CO}_2$ level (Fig. 5b), while no effects of the fluctuating regime at elevated $p\text{CO}_2$ were
268 observed. Dark respiration rates of *T. oceanica* were similar in the steady regimes of ambient and
269 elevated $p\text{CO}_2$ levels. The respiration to net photosynthesis (R:P) ratios for *T. weissflogii* under elevated
270 $p\text{CO}_2$ was higher than at ambient $p\text{CO}_2$ by 73%, while no effects of the fluctuating regime were
271 detected. R:P ratios for *T. oceanica* cells was higher by 104% in the fluctuating regime than for cells in
272 the corresponding steady regime at ambient $p\text{CO}_2$ level (Table 2).

273

274 **4 Discussion**

275 Both species were influenced by elevated $p\text{CO}_2$ in several ways, while they responded differentially
276 to fluctuating regime. In general, for the coastal diatom *T. weissflogii*, the fluctuating $p\text{CO}_2$ regime
277 showed either positive (POC cellular quota and production rate) or no obvious effects on its
278 physiological performance. In contrast, the oceanic diatom *T. oceanica* was significantly negatively
279 affected by the diurnal variation of carbonate chemistry. The fluctuating regime reduced photosynthetic
280 oxygen evolution rates and enhanced dark respiration rates under ambient $p\text{CO}_2$ concentration, while in
281 the OA scenario, the fluctuating regime depressed its growth rate, chlorophyll *a* content, and elemental
282 production rates (which were caused by decreased growth rates).

283 OA depressed the growth of *T. oceanica*, consistent with results of a previous study (King et al.
284 2015), which showed a similar decrease (19%) to the present study (16%). No detectable effects of OA
285 on growth of *T. weissflogii* were found, as reported by previous studies (Burkhardt et al. 1999; Shi et al.
286 2009; Reinfelder 2012; King et al. 2015; Passow and Laws 2015; Taucher et al. 2015). However, the
287 growth responses of diatoms have also been shown to be affected by interactions between OA and other
288 abiotic factors. For instance, the energy saved from active inorganic carbon acquisition mechanisms due

289 to increased availability of CO₂ under OA conditions enhanced the growth of diatoms when daytime
290 mean light level was lower than 22-36% of sea surface solar light intensity. However, growth under OA
291 condition decreased when light exceeded 25-42% of incident irradiance (Gao et al. 2012). OA reduced
292 the growth rate of *T. weissflogii* under light and temperature stress, but no effects of OA were detected
293 in the absence of temperature stress (Passow and Laws 2015). Consequently, it appears that effects of
294 OA on phytoplankton species could be region-specific, depending on the local interactions with other
295 abiotic factors.

296 The silicified cell walls of diatoms act as mechanical protection to resist grazers (Hamm et al. 2003),
297 and also have potential roles in photoprotection (Raven and Waite 2004), as well as promotion of
298 catalysis by extracellular carbonic anhydrase (Milligan and Morel 2002). Si:C ratio of both species
299 decreased under the elevated pCO₂ condition, in accordance with results of Tatters et al. (2012) and
300 Mejia et al. (2013). This decreased ratio indicates that the tested species may fix more carbon per silicon
301 assimilated in the OA scenario than under the ambient pCO₂ condition, and so has implications for
302 changes in local and global carbon and silicon budgets. More carbon may be fixed per diatom cell
303 without changes in silicon quota in the OA scenario, and thus the tested species may contribute more to
304 primary production in the ecosystem, especially in Si-limited waters, in the future oceans. However,
305 diatom silicification is under a complex set of controls. For instance, limitation by other nutrients such
306 as, iron (Hutchins and Bruland 1998) and nitrogen (Flynn and Martin-Jézéquel 2000), may act to
307 increase Si quotas and Si:C ratio.

308 Bicarbonate utilization has been suggested to be a general characteristic of marine diatoms, through
309 direct transport or conversion by extracellular carbonic anhydrase (eCA), while the fraction of direct
310 bicarbonate transport and eCA expression varies among species (Martin and Tortell 2008). Pathways
311 that can utilize HCO₃⁻ and provide CO₂ for Rubisco through C₄ (Reinfelder et al. 2000) or C₃-C₄
312 intermediate photosynthesis (Roberts et al. 2007) have been suggested for *T. weissflogii*. This species
313 takes up both CO₂ and HCO₃⁻ at a similar rate, and has the ability to adjust uptake rates to cope with a
314 wide range of inorganic carbon supplies (Burkhardt et al. 2001). Moreover, *T. weissflogii* has a
315 markedly higher fraction of direct bicarbonate transport and apparent eCA activity than *T. oceanica*

316 (Martin and Tortell 2008), which may facilitate their inorganic carbon transport and uptake. In this
317 study, *T. oceanica* showed significantly lower oxygen evolution rates in the LCf treatment than in the
318 LCs treatment at 11.5 h after the onset of light, when the highest pH and lowest CO₂ was reached. In
319 contrast, no effects of the fluctuating regime on oxygen evolution rates of *T. weissflogii* were found at
320 this time point. Thus *T. weissflogii* cells were more tolerant of the high pH and low CO₂ period under
321 fluctuating carbonate chemistry than *T. oceanica*.

322 Under the fluctuating regime, *T. oceanica* showed higher respiration rates in the current scenario than
323 under the corresponding steady regime. As with the successful compromise between iron requirements
324 and capacity to acclimate to dynamic light regimes in *T. oceanica* cells (Strzepek and Harrison 2004),
325 this oceanic diatom may also have evolved to acclimate to fluctuating carbonate chemistry in a different
326 way compared with the coastal diatom. The higher respiration rate under the fluctuating regime in the
327 current scenario may imply that this species needs more energy for maintaining its intracellular acid-
328 base balance under dynamic extracellular pH conditions, as dark respiration provides energy for growth
329 and metabolic processes (Raven and Beardall, 2005). Diatoms were shown to exhibit circadian
330 variations in photosynthesis and respiration (Weger et al., 1989; Chen and Gao, 2004). Thus dark
331 respiration might show different pattern at other time points, as photosynthetic oxygen evolution did. *T.*
332 *oceanica* cells showed significantly higher R:P ratios than *T. weissflogii*, especially in the fluctuating
333 regime at ambient *p*CO₂, and the ratios were within previously reported ranges in diatoms (Geider and
334 Osborne, 1989). The higher R:P ratio indicated greater proportions of photosynthetic fixed carbon and
335 associated energy were used for growth, biosynthesis, and maintaining intracellular homeostasis in the
336 oceanic species. Moreover, the fluctuating regime reduced the production rate of organic matter by *T.*
337 *oceanica* at elevated *p*CO₂. Depressed biomass build-up has also been found under dynamic light
338 regimes (Wagner et al. 2006; Shatwell et al. 2012; Hoppe et al. 2015). Together with our results, this
339 may imply that organisms that are sensitive to fluctuating abiotic factors maintain intracellular
340 homeostasis under dynamic environments of light or *p*CO₂ at the expense of reduced biomass
341 production.

342 Either positive (POC production rate) or no obvious effects of the fluctuating regime on biomass

343 production were found in the coastal species *T. weissflogii*. Coastal calcifying organisms have shown
344 the ability to achieve homeostasis within critical tissues to facilitate calcification under dynamic
345 pH/pCO₂ condition, and this was suggested to be associated with diurnal and seasonal pH fluctuations
346 in coastal waters (Hendriks et al. 2015). Thus, some organisms could take advantage of the fluctuating
347 carbonate system regime to mitigate the negative effects of ocean acidification on physiological
348 performance. For instance, growth and calcification of corals can benefit from oscillatory pCO₂
349 (Dufault et al. 2012; Comeau et al. 2014). Organisms like *T. weissflogii* whose physiological
350 performance were enhanced or unaltered under dynamic carbonate chemistry conditions thus could be
351 at a distinct advantage in competing with species that showed negative responses to this condition (such
352 as *T. oceanica* in the present study). The differential responses of the tested two species to the
353 fluctuating carbonate chemistry may be partially attributed to the differences in cell size. The
354 differences in carbonate chemistry and pH between the bulk medium and the exterior surface of marine
355 organisms increase as cell size increases (Flynn et al. 2012). Thus the larger species, *T. weissflogii*
356 theoretically possesses higher adaptability to cope with the varied carbonate chemistry and pH, as they
357 are frequently encountered in the natural coastal waters and their exterior surfaces.

358 Schaum et al. (2016) found that short-term plastic responses to high pCO₂ disappeared in a green
359 microalgae after extended experimental evolution at high pCO₂, particularly in fluctuating pCO₂
360 treatments. Whether a similar phenomenon may be operative in other algal groups such as diatoms
361 following exposures to high, fluctuating pCO₂ that are longer than those we employed, is currently
362 unknown. However, it is notable that growth rates and competitive abilities of diatoms of a natural
363 community showed little change following one year of conditioning at two pCO₂ levels and three
364 temperatures, relative to the results of a short-term experiment conducted on the original collected
365 community (Tatters et al. 2013). Regardless of the responses of cell physiology to different timescales
366 of changes in pCO₂ concentrations, it is a significant observation that the fluctuating regime reduced the
367 production rate of organic matter in *T. oceanica* at elevated pCO₂ (which were caused by decreased
368 growth rates).

369 The effect of the fluctuating regime on *T. oceanica* was different in the current and OA scenarios.

370 Under elevated rather than current $p\text{CO}_2$ condition, fluctuating carbonate chemistry decreased pigment
371 content and the production rate of organic matter. Although elevated CO_2 mitigated the negative effects
372 of the fluctuating regime on photosynthetic oxygen evolution rates of *T. oceanica* cells under ambient
373 $p\text{CO}_2$ condition, the effect of the fluctuating regime under elevated $p\text{CO}_2$ tended to be negative,
374 resulting in a decreased growth rate compared to the steady regime. The diurnal pH variation range (\sim
375 0.5 units) used in the present study is realistic for coastal ecosystems, like upwelling regions (Hofmann
376 et al. 2011), kelp forests (Cornwall et al. 2013), coastal coral reefs (Wang et al. 2014), and tide pools
377 (Morris and Taylor, 1983). In contrast, pH in the open ocean is relatively stable, with a variation range
378 of only ~ 0.024 over a month (Hofmann et al. 2011). The same amplitude of pH variation was set in the
379 current and elevated $p\text{CO}_2$ scenarios in the present study. Buffering capacity will decrease as the
380 increase of dissolved inorganic carbon in both coastal and oceanic seawater under projected elevated
381 $p\text{CO}_2$ conditions (Egleston et al. 2010; Cai et al. 2011; Denman et al. 2011; Wang et al. 2013). For
382 instance, the Revelle factor increased from 10.6 ± 0.2 to 15.0 ± 0.2 (a higher Revelle factor indicates a
383 lower buffer capacity) when $p\text{CO}_2$ increased from the ambient to the elevated level in the present study.
384 The increase amplitude of pH variation in coastal water will be more apparent than in oceanic water
385 under an OA scenario, due to high biomass and sufficient nutrients. With a larger diurnal pH variation
386 range in the future ocean, *T. oceanica* would be affected more than observed in the present study. Thus,
387 based on our results, the competitive disadvantage for organisms like *T. oceanica* under fluctuating
388 carbonate chemistry conditions would be amplified in the OA scenario.

389 Given the decreased growth and elemental production rates of *T. oceanica* under fluctuating seawater
390 carbonate chemistry in the OA scenario, and its limited ability to dissipate excess excitation energy
391 through NPQ under high light (Strzepek and Harrison 2004), this species is unlikely to be able to
392 acclimate to coastal habitats, where major fluctuations in light and carbonate chemistry will exist, in the
393 future oceans. In contrast, *T. weissflogii* appears to be insensitive to, even benefit from, fluctuating
394 carbonate chemistry. This striking contrast of physiological traits in coastal and oceanic diatoms
395 suggests that the ability to cope with fluctuating carbonate chemistry may play a role in influencing the
396 geographic distributions of species under OA conditions. It is possible that this ability, together with the

397 abilities to cope with nutrient (Irwin et al. 2006), light (Lavaud et al. 2007; Lavaud and Lepetit 2013;
398 Laviale et al. 2015), and predation pressure (Irigoiien et al. 2005), will determine the spatial distribution
399 patterns of species in the future oceans. However, phytoplankton are known to exhibit species-specific
400 response to environmental factors (including OA, fluctuating carbonate chemistry etc.), thus more
401 studies on the responses of phytoplankton at the species and community levels are needed to predict
402 such broad biogeographic trends.

403

404 **Acknowledgements**

405 We would like to thank the two anonymous reviewers and Dr. Christine Klaas for their insightful
406 comments on the manuscript. This study was supported by State Oceanic Administration (SOA, GASI-
407 03-01-02-04), National Natural Science Foundation (41430967, 41120164007, 41206091), Joint project
408 of NSFC and Shandong province (Grant No. U1406403), Strategic Priority Research Program of
409 Chinese Academy of Sciences (Grant No. XDA11020302), the Fundamental Research Funds for the
410 Central Universities (20720150076), and U.S. National Science Foundation grant OCE 1538525 to F-
411 X.F. and D.A.H. We thank Prof. John Beardall for his suggestions to experimental design and Prof.
412 Dalin Shi for providing *Thalassiosira weissflogii*. We are grateful to Hangbin Miao and Dong Yan for
413 their help with the experiments.

414 **References**

- 415 Britton, D., Cornwall, C. E., Revill, A. T., Hurd, C. L., and Johnson, C. R.: Ocean acidification reverses
416 the positive effects of seawater pH fluctuations on growth and photosynthesis of the habitat-forming
417 kelp, *Ecklonia radiata*, Scientific Reports, 6, 26036, doi:10.1038/srep26036, 2016.
- 418 Brzezinski, M. A., and Nelson, D. M.: The annual silica cycle in the Sargasso Sea near Bermuda, Deep-
419 Sea Res. Part I, 42, 1215-1237, 1995.
- 420 Burkhardt, S., Zondervan, I., and Riebesell, U.: Effect of CO₂ concentration on C: N: P ratio in marine
421 phytoplankton: A species comparison, Limnol. Oceanogr., 44, 683-690, 1999.
- 422 Burkhardt, S., Amoroso, G., Riebesell, U., and Sültemeyer, D.: CO₂ and HCO₃⁻ uptake in marine
423 diatoms acclimated to different CO₂ concentrations, Limnol. Oceanogr., 46, 1378-1391, 2001.
- 424 Cai, W.-J., Hu, X., Huang, W.-J., Murrell, M. C., Lehrter, J. C., Lohrenz, S. E., Chou, W.-C., Zhai, W.,
425 Hollibaugh, J. T., and Wang, Y.: Acidification of subsurface coastal waters enhanced by
426 eutrophication, Nat. Geosci., 4, 766-770, 2011.
- 427 Capone, D. G., and Hutchins, D. A.: Microbial biogeochemistry of coastal upwelling regimes in a
428 changing ocean, Nat. Geosci., 6, 711-717, 2013.
- 429 Chen, X. and Gao, K.: Characterization of diurnal photosynthetic rhythms in the marine diatom
430 *Skeletonema costatum* grown in synchronous culture under ambient and elevated CO₂, Funct. Plant.
431 Biol., 31, 399-404, 2004.
- 432 Ciais, P., Sabine, C., Bala, G., Bopp, L., Brovkin, V., Canadell, J., Chhabra, A., DeFries, R., Galloway,
433 J., and Heimann, M.: Carbon and other biogeochemical cycles, in: Climate change 2013: the physical
434 science basis. Contribution of Working Group I to the Fifth Assessment Report of the
435 Intergovernmental Panel on Climate Change, Cambridge University Press, 465-570, 2014.
- 436 Comeau, S., Edmunds, P. J., Spindel, N. B., and Carpenter, R. C.: Diel pCO₂ oscillations modulate the
437 response of the coral *Acropora hyacinthus* to ocean acidification, Mar. Ecol. Prog. Ser., 501, 99-111,
438 2014.
- 439 Cornwall, C. E., Hepburn, C. D., McGraw, C. M., Currie, K. I., Pilditch, C. A., Hunter, K. A., Boyd, P.
440 W., and Hurd, C. L.: Diurnal fluctuations in seawater pH influence the response of a calcifying

441 macroalga to ocean acidification, P. Roy. Soc. Lond. B Bio., 280, 20132201,
442 doi:10.1098/rspb.2013.2201, 2013.

443 Dai, M., Lu, Z., Zhai, W., Chen, B., Cao, Z., Zhou, K., Cai, W. J., and Chenc, C. T. A.: Diurnal
444 variations of surface seawater $p\text{CO}_2$ in contrasting coastal environments, *Limnol. Oceanogr.*, 54,
445 735-745, 2009.

446 Denman, K., Christian, J. R., Steiner, N., Pörtner, H.-O., and Nojiri, Y.: Potential impacts of future
447 ocean acidification on marine ecosystems and fisheries: current knowledge and recommendations for
448 future research, *ICES J. Mar. Sci.*, 68, 1019-1029, 2011.

449 Dixon, R. L.: Behavioral responses of common juvenile estuarine fishes to diel-cycling hypoxia and
450 corresponding pH fluctuations: a comparative approach, Ph.D. thesis, University of Delaware, USA,
451 2014.

452 Doney, S. C.: The growing human footprint on coastal and open-ocean biogeochemistry, *Science*, 328,
453 1512-1516, 2010.

454 Drupp, P., De Carlo, E. H., Mackenzie, F. T., Bienfang, P., and Sabine, C. L.: Nutrient inputs,
455 phytoplankton response, and CO_2 variations in a semi-enclosed subtropical embayment, Kaneohe
456 Bay, Hawaii, *Aquat. Geochem.*, 17, 473-498, 2011.

457 Duarte, C. M., Hendriks, I. E., Moore, T. S., Olsen, Y. S., Steckbauer, A., Ramajo, L., Carstensen, J.,
458 Trotter, J. A., and McCulloch, M.: Is ocean acidification an open-ocean syndrome? Understanding
459 anthropogenic impacts on seawater pH, *Estuar. Coast.*, 36, 221-236, 2013.

460 Dufault, A. M., Cumbo, V. R., Fan, T.-Y., and Edmunds, P. J.: Effects of diurnally oscillating $p\text{CO}_2$ on
461 the calcification and survival of coral recruits, *P. Roy. Soc. B Biol. Sci.*, 279, 2951-2958, 2012.

462 Egleston, E. S., Sabine, C. L., and Morel, F. M.: Revelle revisited: Buffer factors that quantify the
463 response of ocean chemistry to changes in DIC and alkalinity, *Global Biogeochem. Cy.*, 24, 2010.

464 Feely, R. A., Sabine, C. L., Hernandez-Ayon, J. M., Ianson, D., and Hales, B.: Evidence for upwelling
465 of corrosive" acidified" water onto the continental shelf, *Science*, 320, 1490-1492, 2008.

466 Flynn, K. J., and Martin-Jézéquel, V.: Modelling Si–N-limited growth of diatoms, *J. Plankton Res.*, 22,
467 447-472, 2000.

468 Flynn, K. J., Blackford, J. C., Baird, M. E., Raven, J. A., Clark, D. R., Beardall, J., Brownlee, C.,
469 Fabian, H., and Wheeler, G. L.: Changes in pH at the exterior surface of plankton with ocean
470 acidification, *Nature Climate Change*, 2, 510-513, 2012.

471 Frieder, C. A., Gonzalez, J. P., Bockmon, E. E., Navarro, M. O., and Levin, L. A.: Can variable pH and
472 low oxygen moderate ocean acidification outcomes for mussel larvae?, *Global Change Biol.*, 20,
473 754-764, 2014.

474 Gao, K., Aruga, Y., Asada, K., Ishihara, T., Akano, T., and Kiyohara, M.: Calcification in the articulated
475 coralline alga *Corallina pilulifera*, with special reference to the effect of elevated CO₂ concentration,
476 *Mar. Biol.*, 117, 129-132, 1993.

477 Gao, K., Xu, J., Gao, G., Li, Y., Hutchins, D. A., Huang, B., Wang, L., Zheng, Y., Jin, P., and Cai, X.:
478 Rising CO₂ and increased light exposure synergistically reduce marine primary productivity, *Nature*
479 *Climate Change*, 2, 519-523, 2012.

480 Gattuso, J.-P., Frankignoulle, M., and Wollast, R.: Carbon and carbonate metabolism in coastal aquatic
481 ecosystems, *Annu. Rev. Ecol. Syst.*, 405-434, 1998.

482 Gattuso, J.-P., Magnan, A., Billé, R., Cheung, W., Howes, E., Joos, F., Allemand, D., Bopp, L., Cooley,
483 S., and Eakin, C.: Contrasting futures for ocean and society from different anthropogenic CO₂
484 emissions scenarios, *Science*, 349, aac4722, doi:10.1126/science.aac4722, 2015.

485 Geider, R. J., and Osborne, B. A.: Respiration and microalgal growth: a review of the quantitative
486 relationship between dark respiration and growth, *New Phytol.*, 112, 327-341, 1989.

487 Genty, B., Briantais, J.-M., and Baker, N. R.: The relationship between the quantum yield of
488 photosynthetic electron transport and quenching of chlorophyll fluorescence, *BBA Gen. Subjects*,
489 990, 87-92, 1989.

490 Glibert, P., and Ray, R.: Different patterns of growth and nitrogen uptake in two clones of marine
491 *Synechococcus* spp, *Mar. Biol.*, 107, 273-280, 1990.

492 Hamm, C. E., Merkel, R., Springer, O., Jurkojc, P., Maier, C., Prechtel, K., and Smetacek, V.:
493 Architecture and material properties of diatom shells provide effective mechanical protection,
494 *Nature*, 421, 841-843, 2003.

495 Hendriks, I. E., Duarte, C. M., Olsen, Y. S., Steckbauer, A., Ramajo, L., Moore, T. S., Trotter, J. A., and
496 McCulloch, M.: Biological mechanisms supporting adaptation to ocean acidification in coastal
497 ecosystems, *Estuar. Coast. Shelf S.*, 152, A1-A8, doi:10.1016/j.ecss.2014.07.019, 2015.

498 Hofmann, G. E., Smith, J. E., Johnson, K. S., Send, U., Levin, L. A., Micheli, F., Paytan, A., Price, N.
499 N., Peterson, B., and Takeshita, Y.: High-frequency dynamics of ocean pH: a multi-ecosystem
500 comparison, *PloS One*, 6, e28983, doi: 10.1371/journal.pone.0028983, 2011.

501 Hoppe, C. J., Holtz, L. M., Trimborn, S., and Rost, B.: Ocean acidification decreases the light-use
502 efficiency in an Antarctic diatom under dynamic but not constant light, *New Phytol.*, 207 (1), 159-
503 171, 2015.

504 Howes, E. L., Joos, F., Eakin, M., and Gattuso, J.: An updated synthesis of the observed and projected
505 impacts of climate change on the chemical, physical and biological processes in the oceans, *Frontiers*
506 *in Marine Science*, 2, 36, doi:10.3389/fmars.2015.00036, 2015.

507 Hurd, C. L., Cornwall, C. E., Currie, K., Hepburn, C. D., McGraw, C. M., Hunter, K. A., and Boyd, P.
508 W.: Metabolically induced pH fluctuations by some coastal calcifiers exceed projected 22nd century
509 ocean acidification: a mechanism for differential susceptibility?, *Global Change Biol.*, 17, 3254-
510 3262, 2011.

511 Hutchins, D. A., and Bruland, K. W.: Iron-limited diatom growth and Si: N uptake ratios in a coastal
512 upwelling regime, *Nature*, 393, 561-564, 1998.

513 Irigoien, X., Flynn, K., and Harris, R.: Phytoplankton blooms: a 'loophole' in microzooplankton grazing
514 impact?, *J. Plankton Res.*, 27, 313-321, 2005.

515 Irwin, A. J., Finkel, Z. V., Schofield, O. M. E., and Falkowski, P. G.: Scaling-up from nutrient
516 physiology to the size-structure of phytoplankton communities, *J. Plankton Res.*, 28, 459-471, 2006.

517 Jiang, Z.-P., Huang Jr, -. C., Dai, M., Kao, S. J., Hydes, D. J., Chou, W.-C., and Jan, S.: Short-term
518 dynamics of oxygen and carbon in productive nearshore shallow seawater systems off Taiwan:
519 Observations and modeling, *Limnol. Oceanogr.*, 56, 1832-1849, 2011.

520 Johnson, M. D., Moriarty, V. W., and Carpenter, R. C.: Acclimatization of the crustose coralline alga
521 *Porolithon onkodes* to variable $p\text{CO}_2$, *PloS One*, 9, e87678, doi:10.1371/journal.pone.0087678,

522 2014.

523 Keppel, A. G., Breitburg, D. L., Wikfors, G. H., Burrell, R. B., and Clark, V. M.: Effects of co-varying
524 diel-cycling hypoxia and pH on disease susceptibility in the eastern oyster, *Crassostrea virginica*,
525 Mar. Ecol. Prog. Ser., 538, 169-183, 2015.

526 King, A. L., Jenkins, B. D., Wallace, J. R., Liu, Y., Wikfors, G. H., Milke, L. M., and Meseck, S. L.:
527 Effects of CO₂ on growth rate, C: N: P, and fatty acid composition of seven marine phytoplankton
528 species, Mar. Ecol. Prog. Ser., 537, 59-69, 2015.

529 Lavaud, J., Strzepek, R. F., and Kroth, P. G.: Photoprotection capacity differs among diatoms: Possible
530 consequences on the spatial distribution of diatoms related to fluctuations in the underwater light
531 climate, Limnol. Oceanogr., 52, 1188-1194, 2007.

532 Lavaud, J., and Lepetit, B.: An explanation for the inter-species variability of the photoprotective non-
533 photochemical chlorophyll fluorescence quenching in diatoms, BBA Bioenergetics, 1827, 294-302,
534 2013.

535 Laviale, M., Barnett, A., Ezequiel, J., Lepetit, B., Frankenbach, S., Méléder, V., Serôdio, J., and Lavaud,
536 J.: Response of intertidal benthic microalgal biofilms to a coupled light–temperature stress: evidence
537 for latitudinal adaptation along the Atlantic coast of Southern Europe, Environ. Microbiol., 17 (10),
538 3662-3677, 2015.

539 Li, G., Gao, K., and Gao, G.: Differential impacts of solar UV radiation on photosynthetic carbon
540 fixation from the coastal to offshore surface waters in the South China Sea, Photochem. Photobiol.,
541 87, 329-334, 2011.

542 Liu, S.-W., and Qiu, B.-S.: Different responses of photosynthesis and flow cytometric signals to iron
543 limitation and nitrogen source in coastal and oceanic *Synechococcus* strains (Cyanophyceae), Mar.
544 Biol., 159, 519-532, 2012.

545 Martin, C. L., and Tortell, P. D.: Bicarbonate transport and extracellular carbonic anhydrase in marine
546 diatoms, Physiol. Plantarum, 133, 106-116, 2008.

547 Mejia, L. M., Isensee, K., Méndez-Vicente, A., Pisonero, J., Shimizu, N., González, C., Monteleone, B.,
548 and Stoll, H.: B content and Si/C ratios from cultured diatoms (*Thalassiosira pseudonana* and

549 *Thalassiosira weissflogii*): Relationship to seawater pH and diatom carbon acquisition, *Geochim.*
550 *Cosmochim. Ac.*, 123, 322-337, 2013.

551 Milligan, A. J., and Morel, F. M.: A proton buffering role for silica in diatoms, *Science*, 297, 1848-1850,
552 2002.

553 Morris, S. and Taylor, A. C.: Diurnal and seasonal variation in physico-chemical conditions within
554 intertidal rock pools, *Estuar. Coast. Shelf S.*, 17, 339-355, 1983.

555 Noisette, F., Egilsdottir, H., Davoult, D., and Martin, S.: Physiological responses of three temperate
556 coralline algae from contrasting habitats to near-future ocean acidification, *J. Exp. Mar. Biol. Ecol.*,
557 448, 179-187, 2013.

558 Onitsuka, T., Kimura, R., Ono, T., Takami, H., and Nojiri, Y.: Effects of ocean acidification on the early
559 developmental stages of the horned turban, *Turbo cornutus*, *Mar. Biol.*, 161, 1127-1138, 2014.

560 Orr, J. C., Fabry, V. J., Aumont, O., Bopp, L., Doney, S. C., Feely, R. A., Gnanadesikan, A., Gruber, N.,
561 Ishida, A., and Joos, F.: Anthropogenic ocean acidification over the twenty-first century and its
562 impact on calcifying organisms, *Nature*, 437, 681-686, 2005.

563 Passow, U., and Laws, E. A.: Ocean acidification as one of multiple stressors: growth response of
564 *Thalassiosira weissflogii* (diatom) under temperature and light stress, *Mar. Ecol. Prog. Ser.*, 541, 75-
565 90, 2015.

566 Raven, J. A. and Beardall, J.: Respiration in aquatic photolithotrophs, in: *Respiration in aquatic*
567 *ecosystems*, edited by: del Giorgio, P. A. and Williams, P.J. le B., Oxford University Press, New
568 York, USA, 36-46, 2005.

569 Raven, J., and Waite, A.: The evolution of silicification in diatoms: inescapable sinking and sinking as
570 escape?, *New Phytol.*, 162, 45-61, 2004.

571 Reinfelder, J. R., Kraepiel, A. M., and Morel, F. M.: Unicellular C₄ photosynthesis in a marine diatom,
572 *Nature*, 407, 996-999, 2000.

573 Reinfelder, J. R.: Carbon dioxide regulation of nitrogen and phosphorus in four species of marine
574 phytoplankton, *Mar. Ecol. Prog. Ser.*, 466, 57-67, 2012.

575 Ritchie, R. J.: Consistent sets of spectrophotometric chlorophyll equations for acetone, methanol and

576 ethanol solvents, *Photosynth. Res.*, 89, 27-41, 2006.

577 Roberts, K., Granum, E., Leegood, R. C., and Raven, J. A.: Carbon acquisition by diatoms, *Photosynth.*
578 *Res.*, 93, 79-88, 2007.

579 Sabine, C. L., Feely, R. A., Gruber, N., Key, R. M., Lee, K., Bullister, J. L., Wanninkhof, R., Wong, C.,
580 Wallace, D. W., and Tilbrook, B.: The oceanic sink for anthropogenic CO₂, *Science*, 305, 367-371,
581 2004.

582 Schaum, C.-E., Rost, B., and Collins, S.: Environmental stability affects phenotypic evolution in a
583 globally distributed marine picoplankton, *ISME J.*, 10, 75-84, 2015.

584 Shatwell, T., Nicklisch, A., and Köhler, J.: Temperature and photoperiod effects on phytoplankton
585 growing under simulated mixed layer light fluctuations, *Limnol. Oceanogr.*, 57, 541-553, 2012.

586 Shi, D., Xu, Y., and Morel, F.: Effects of the pH/pCO₂ control method on medium chemistry and
587 phytoplankton growth, *Biogeosciences*, 6, 1199-1207, 2009.

588 Strzepek, R. F., and Harrison, P. J.: Photosynthetic architecture differs in coastal and oceanic diatoms,
589 *Nature*, 431, 689-692, 2004.

590 Sunda, W. G., Price, N. M., and Morel, F. M.: Trace metal ion buffers and their use in culture studies, in:
591 *Algal culturing techniques*, Elsevier Academic Press, 35-63, 2005.

592 Tatters, A. O., Fu, F.-X., and Hutchins, D. A.: High CO₂ and silicate limitation synergistically increase
593 the toxicity of *Pseudo-nitzschia fraudulenta*, *PloS One*, 7, e32116,
594 doi:10.1371/journal.pone.0032116, 2012.

595 Tatters, A. O., Roleda, M. Y., Schnetzer, A., Fu, F., Hurd, C. L., Boyd, P. W., Caron, D. A., Lie, A. A.,
596 Hoffmann, L. J., and Hutchins, D. A.: Short-and long-term conditioning of a temperate marine
597 diatom community to acidification and warming, *Philos. T. Roy. Soc. B*, 368, 20120437,
598 doi:10.1098/rstb.2012.0437, 2013.

599 Taucher, J., Jones, J., James, A., Brzezinski, M. A., Carlson, C. A., Riebesell, U., and Passow, U.:
600 Combined effects of CO₂ and temperature on carbon uptake and partitioning by the marine diatoms
601 *Thalassiosira weissflogii* and *Dactyliosolen fragilissimus*, *Limnol. Oceanogr.*, 60, 901-919, 2015.

602 Wagner, H., Jakob, T., and Wilhelm, C.: Balancing the energy flow from captured light to biomass under

603 fluctuating light conditions, *New Phytol.*, 169, 95-108, 2006.

604 Waldbusser, G. G., and Salisbury, J. E.: Ocean acidification in the coastal zone from an organism's
605 perspective: multiple system parameters, frequency domains, and habitats, *Annual Review of Marine*
606 *Science*, 6, 221-247, 2014.

607 Wang, G., Jing, W., Wang, S., Xu, Y., Wang, Z., Zhang, Z., Li, Q., and Dai, M.: Coastal acidification
608 induced by tidal-driven submarine groundwater discharge in a coastal coral reef system, *Environ.*
609 *Sci. Technol.*, 48, 13069-13075, 2014.

610 Wang, Z. A., Wanninkhof, R., Cai, W.-J., Byrne, R. H., Hu, X., Peng, T.-H., and Huang, W.-J.: The
611 marine inorganic carbon system along the Gulf of Mexico and Atlantic coasts of the United States:
612 Insights from a transregional coastal carbon study, *Limnol. Oceanogr.*, 58, 325-342, 2013.

613 Weger, H. G., Herzig, R., Falkowski, P. G., and Turpin, D. H.: Respiratory losses in the light in a marine
614 diatom: Measurements by short-term mass spectrometry, *Limnol. Oceanogr.*, 34, 1153-1161, 1989.

615

616

617 **Figure captions**

618 Figure 1. Measured pH_{NBS} variation over a diel cycle in the four experimental treatments (LCs, closed
619 triangles; LCf, open triangles; HCs, closed circles; HCF, open circles). Here pH values of triplicate
620 cultures in one experimental day are shown.

621

622 Figure 2. Specific growth rates of *T. weissflogii* (a) and *T. oceanica* (b) under steady (closed bars) and
623 fluctuating (open bars) regimes of ambient (LC) and elevated (HC) $p\text{CO}_2$ levels. Values are means \pm SD
624 of triplicate cultures. The different letters indicate significant ($p < 0.05$) differences among treatments.

625

626 Figure 3. Production rates of chlorophyll *a* (a, b), POC (c, d), PON (e, f), and BSi (g, h) of *T. weissflogii*
627 (a, c, e, g) and *T. oceanica* (b, d, f, h) under steady (closed bars) and fluctuating (open bars) regimes of
628 ambient (LC) and elevated (HC) $p\text{CO}_2$ levels. Values are means \pm SD of triplicate cultures. The
629 different letters indicate significant ($p < 0.05$) differences among treatments.

630

631 Figure 4. Chlorophyll-normalized net oxygen evolution rates determined at 6 h after the onset of light
632 for *T. weissflogii* (a) and *T. oceanica* (b) under steady (closed bars) and fluctuating (open bars) regimes
633 of ambient (LC) and elevated (HC) $p\text{CO}_2$ levels. Oxygen evolution rates per cell of *T. weissflogii* (c)
634 and *T. oceanica* (d) of the four treatments determined 0.5, 6, and 11.5 h after the onset of light. Values
635 are means \pm SD of triplicate cultures. The different letters indicate significant ($p < 0.05$) differences
636 among treatments.

637

638 Figure 5. Dark respiration rates determined at 6 h after the onset of light for *T. weissflogii* (a) and *T.*
639 *oceanica* (b) under steady (closed bars) and fluctuating (open bars) regimes of ambient (LC) and
640 elevated (HC) $p\text{CO}_2$ levels. Values are means \pm SD of triplicate cultures. The different letters indicate
641 significant ($p < 0.05$) differences among treatments.

642

643

644 Table 1. Carbonate chemistry parameters of culture media before and after dilution under steady and fluctuating regimes of ambient (LC) and elevated
 645 (HC) $p\text{CO}_2$ levels. Values are means \pm SD of triplicate cultures. The different letters indicate significant ($p < 0.05$) differences among treatments.

646

	pH_{NBS}	TA ($\mu\text{mol kg}^{-1}$)	DIC ($\mu\text{mol kg}^{-1}$)	HCO_3^- ($\mu\text{mol kg}^{-1}$)	CO_3^{2-} ($\mu\text{mol kg}^{-1}$)	CO_2 ($\mu\text{mol kg}^{-1}$)
After dilution						
LCs	8.12 ± 0.03^a	2397 ± 7^a	2132 ± 20^a	1929 ± 27^a	188 ± 8^a	16 ± 1^a
LCf	8.13 ± 0.01^a	2398 ± 2^a	2128 ± 6^a	1922 ± 10^a	191 ± 4^a	15 ± 1^a
HCs	7.80 ± 0.02^b	2392 ± 5^a	2279 ± 10^b	2144 ± 12^b	98 ± 3^b	37 ± 1^b
HCf	7.80 ± 0.02^b	2406 ± 13^a	2288 ± 19^b	2152 ± 20^b	100 ± 3^b	36 ± 2^b
Before dilution						
LCs	8.13 ± 0.02^a	2399 ± 2^a	2133 ± 7^a	1929 ± 12^a	189 ± 5^a	15 ± 1^a
LCf	8.14 ± 0.02^a	2388 ± 19^a	2116 ± 21^a	1910 ± 22^a	191 ± 5^a	15 ± 1^a
HCs	7.79 ± 0.02^b	2401 ± 6^a	2287 ± 7^b	2153 ± 8^b	98 ± 4^b	37 ± 2^b
HCf	7.82 ± 0.01^b	2408 ± 9^a	2283 ± 12^b	2144 ± 13^b	104 ± 2^b	34 ± 1^b

647

648

649

650

651

652

653 Table 2. Cell size, respiration to photosynthesis ratio (R:P), cellular quotas of chlorophyll, particulate organic carbon (POC), particulate organic nitrogen
 654 (PON), and biogenic silica (BSi) and elemental ratios of *T. weissflogii* and *T. oceanica* under steady and fluctuating regimes of ambient (LC) and elevated
 655 (HC) $p\text{CO}_2$ levels. Values are means \pm SD of triplicate cultures. The different letters indicate significant ($p < 0.05$) differences among treatments.

656

	<i>T. weissflogii</i>				<i>T. oceanica</i>			
	LCs	LCf	HCs	HCf	LCs	LCf	HCs	HCf
Cell size (μm)	12.17 \pm 0.05 ^a	12.17 \pm 0.05 ^a	12.20 \pm 0.04 ^a	12.18 \pm 0.04 ^a	5.58 \pm 0.01 ^A	5.65 \pm 0.03 ^B	5.71 \pm 0.02 ^C	5.63 \pm 0.02 ^B
Cellular quotas								
Chl <i>a</i> (pg cell ⁻¹)	3.24 \pm 0.14 ^a	3.15 \pm 0.05 ^a	3.25 \pm 0.05 ^a	3.27 \pm 0.07 ^a	0.30 \pm 0.03 ^A	0.33 \pm 0.02 ^{AB}	0.38 \pm 0.06 ^B	0.29 \pm 0.02 ^A
POC (pmol cell ⁻¹)	6.94 \pm 0.36 ^a	7.59 \pm 0.23 ^b	10.28 \pm 0.29 ^c	10.28 \pm 0.28 ^c	1.49 \pm 0.12 ^A	1.68 \pm 0.20 ^A	2.38 \pm 0.17 ^B	2.20 \pm 0.07 ^B
PON (pmol cell ⁻¹)	1.21 \pm 0.14 ^a	1.34 \pm 0.12 ^a	1.94 \pm 0.11 ^b	1.80 \pm 0.06 ^b	0.25 \pm 0.03 ^A	0.29 \pm 0.01 ^A	0.49 \pm 0.03 ^B	0.44 \pm 0.03 ^B
BSi (pmol cell ⁻¹)	1.11 \pm 0.01 ^{ab}	1.06 \pm 0.04 ^a	1.19 \pm 0.10 ^b	1.04 \pm 0.04 ^a	0.35 \pm 0.03 ^A	0.34 \pm 0.03 ^A	0.32 \pm 0.02 ^{AB}	0.29 \pm 0.01 ^B
Ratios								
C:N (pmol:pmol)	5.78 \pm 0.40 ^a	5.68 \pm 0.32 ^a	5.30 \pm 0.20 ^a	5.72 \pm 0.24 ^a	6.10 \pm 0.60 ^A	5.87 \pm 0.70 ^{AB}	4.90 \pm 0.16 ^B	5.05 \pm 0.36 ^B
Si:C (pmol:pmol)	0.16 \pm 0.01 ^a	0.14 \pm 0.01 ^b	0.12 \pm 0.01 ^c	0.10 \pm 0.01 ^c	0.24 \pm 0.02 ^A	0.20 \pm 0.02 ^B	0.14 \pm 0.01 ^C	0.13 \pm 0.01 ^C
R:P (fmol cell ⁻¹ h ⁻¹ : fmol cell ⁻¹ h ⁻¹)	0.08 \pm 0.01 ^a	0.08 \pm 0.02 ^a	0.13 \pm 0.03 ^b	0.14 \pm 0.03 ^b	0.27 \pm 0.07 ^A	0.55 \pm 0.12 ^B	0.29 \pm 0.06 ^A	0.39 \pm 0.04 ^A

657

658

659

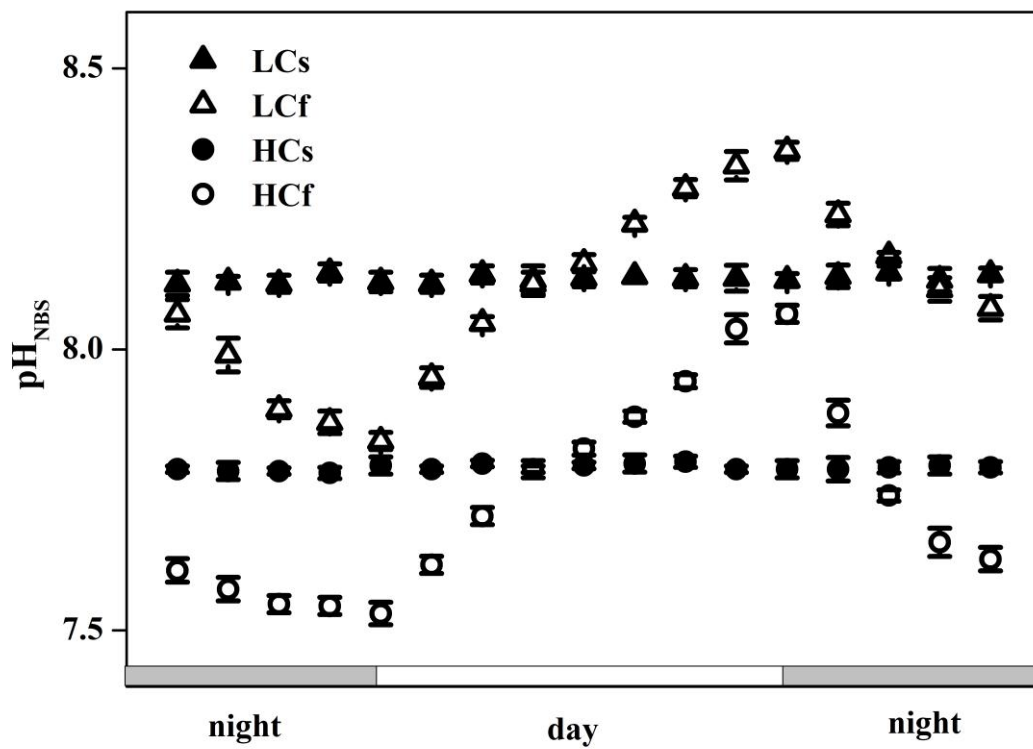
660 Table 3. Effective photochemical quantum yields (Φ_{PSII}) and non-photochemical quenching (NPQ) determined 0.5, 6, and 11.5 h after the onset of light of
661 *T. weissflogii* and *T. oceanica* under steady and fluctuating regimes of ambient (LC) and elevated (HC) $p\text{CO}_2$ levels. Φ_{PSII} and NPQ were determined under
662 actinic light intensity ($\sim 156 \mu\text{mol photons m}^{-2} \text{s}^{-1}$) similar to culture light level after 10 min dark adaptation. Values are means \pm SD of triplicate cultures.
663 The different letters indicate significant ($p < 0.05$) differences among treatments.

664

		<i>T. weissflogii</i>				<i>T. oceanica</i>			
	Time point	LCs	LCf	HCs	HCf	LCs	LCf	HCs	HCf
Φ_{PSII}	0.5 h	0.61 \pm 0.01 ^a	0.61 \pm 0.01 ^a	0.59 \pm 0.01 ^a	0.54 \pm 0.03 ^b	0.57 \pm 0.03 ^A	0.58 \pm 0.01 ^A	0.59 \pm 0.06 ^A	0.61 \pm 0.03 ^A
	6 h	0.60 \pm 0.01 ^a	0.60 \pm 0.01 ^a	0.58 \pm 0.01 ^b	0.59 \pm 0.01 ^b	0.57 \pm 0.01 ^A	0.57 \pm 0.01 ^A	0.54 \pm 0.01 ^B	0.56 \pm 0.01 ^{AB}
	11.5 h	0.58 \pm 0.01 ^a	0.58 \pm 0.01 ^a	0.57 \pm 0.01 ^b	0.57 \pm 0.01 ^{ab}	0.61 \pm 0.03 ^A	0.60 \pm 0.03 ^{AB}	0.57 \pm 0.01 ^B	0.57 \pm 0.01 ^{AB}
NPQ	0.5 h	0.13 \pm 0.02 ^a	0.13 \pm 0.01 ^a	0.13 \pm 0.01 ^a	0.23 \pm 0.05 ^b	0.10 \pm 0.02 ^A	0.06 \pm 0.02 ^A	0.08 \pm 0.05 ^A	0.12 \pm 0.09 ^A
	6 h	0.08 \pm 0.03 ^a	0.08 \pm 0.02 ^{ab}	0.11 \pm 0.01 ^b	0.09 \pm 0.01 ^{ab}	0.13 \pm 0.02 ^A	0.14 \pm 0.01 ^A	0.18 \pm 0.02 ^B	0.19 \pm 0.01 ^B
	11.5 h	0.08 \pm 0.01 ^a	0.07 \pm 0.01 ^a	0.06 \pm 0.01 ^b	0.07 \pm 0.01 ^{ab}	0.09 \pm 0.02 ^A	0.06 \pm 0.01 ^B	0.06 \pm 0.01 ^B	0.07 \pm 0.01 ^{AB}

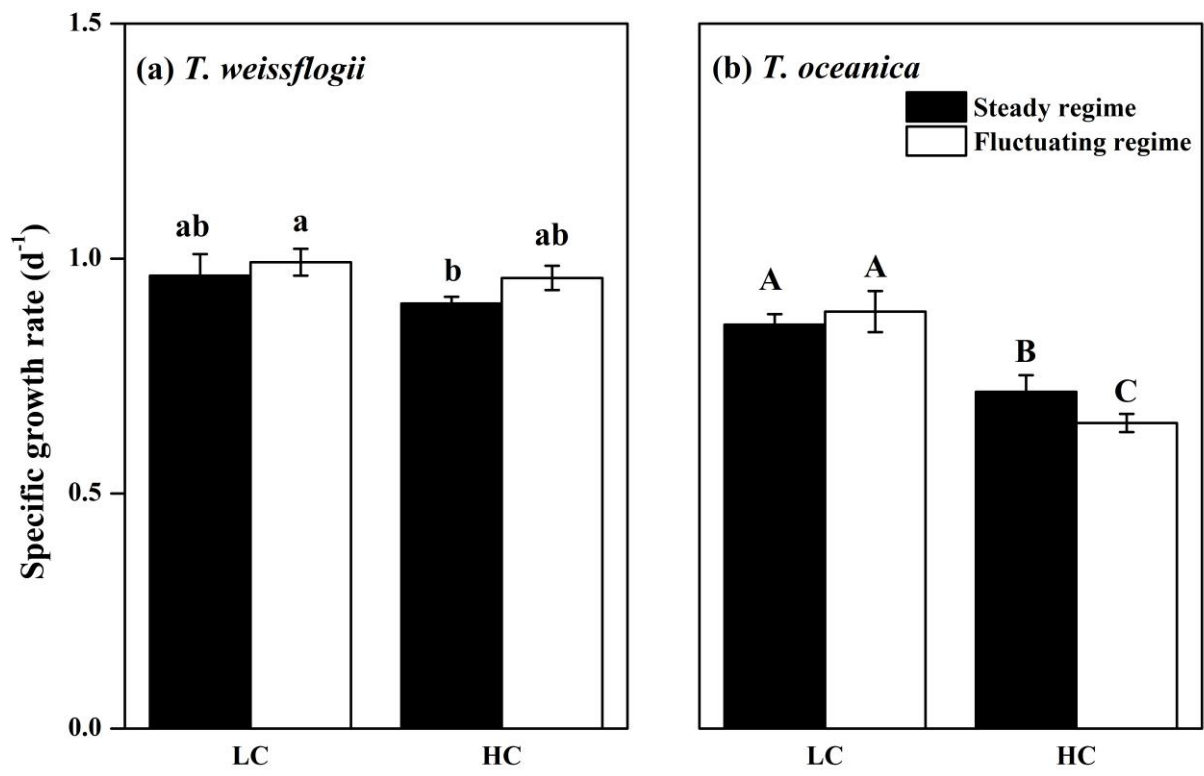
665

666
667
668



669
670
671

Figure 1



672

673

674

Figure 2

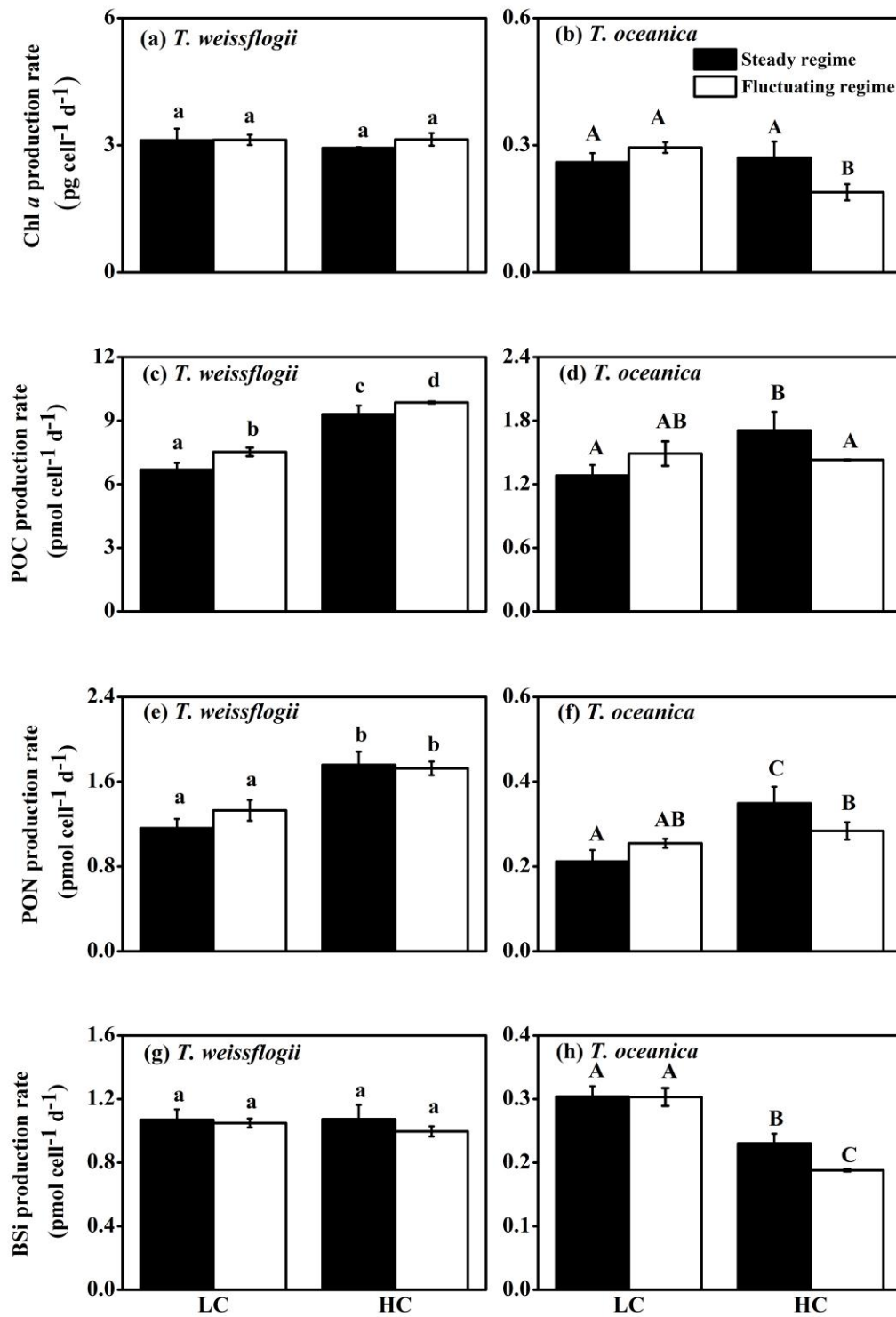
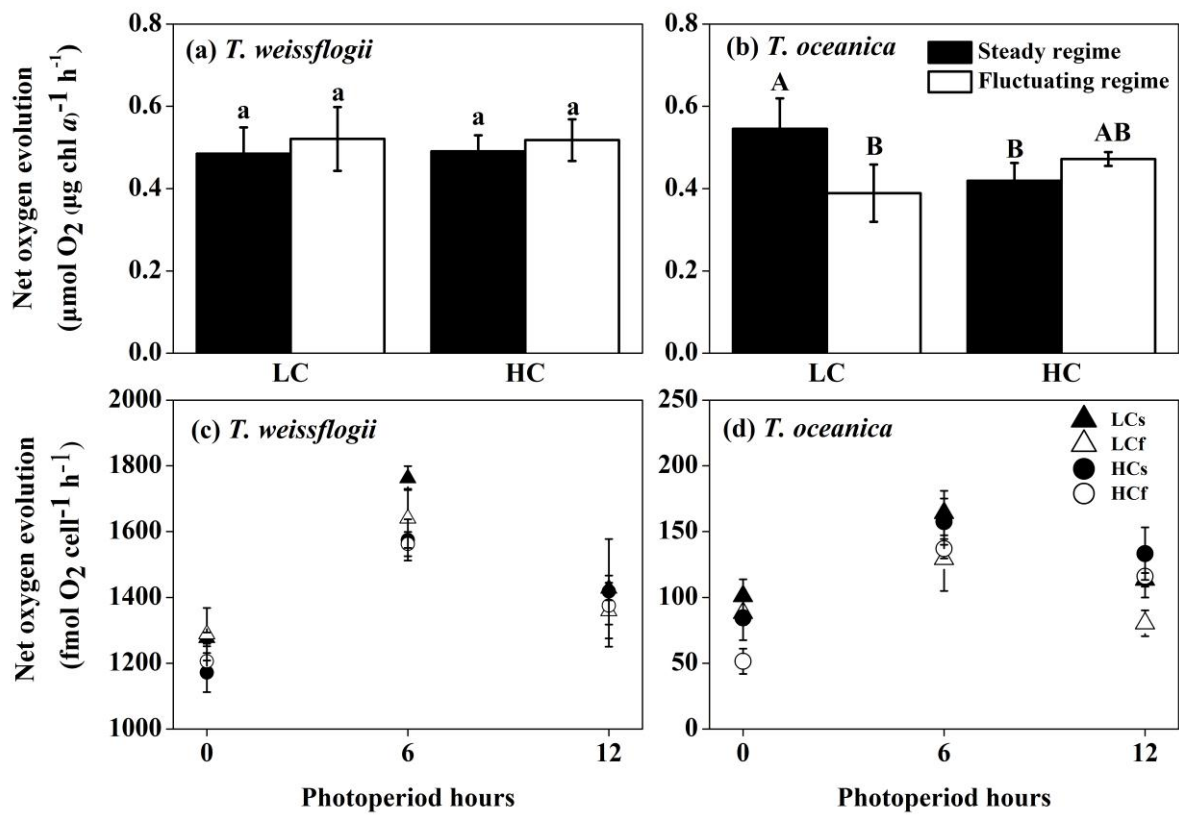


Figure 3

675

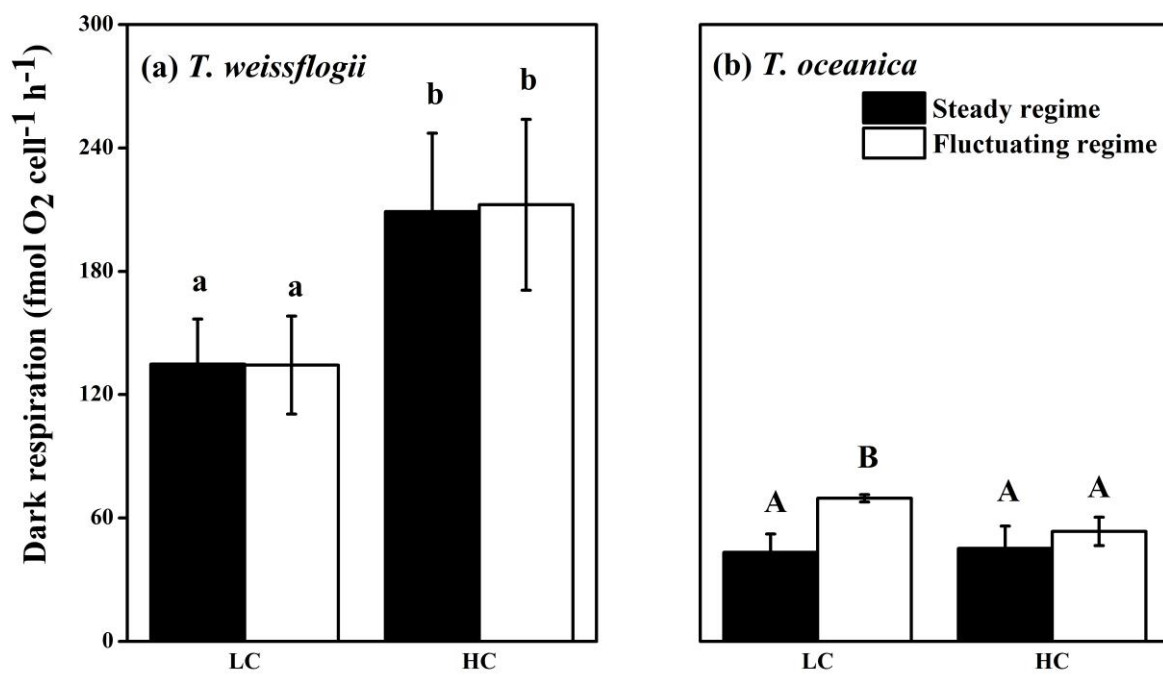
676



677

678

Figure 4



679

680

681

Figure 5